J. Cell. Mol. Med. Vol 13, No 9B, 2009 pp. 3236-3250

Potential for control of detrusor smooth muscle spontaneous rhythmic contraction by cyclooxygenase products released by interstitial cells of Cajal

Clinton Collins [a, #], Adam P. Klausner [a, #], Benjamin Herrick [a], Harry P. Koo [a], Amy S. Miner [b, c], Scott C. Henderson [d] Paul H. Ratz [b, c, *]

[a] Department of Surgery, Urology Division, Virginia Commonwealth University School of Medicine, VA, USA
[b] Departments of Biochemistry & Molecular Biology, Virginia Commonwealth University School of Medicine, VA, USA
[c] Department of Pediatrics, Virginia Commonwealth University School of Medicine, VA, USA
[d] Department of Anatomy and Neurobiology, Virginia Commonwealth University School of Medicine, VA, USA

Received: July 14, 2008; Accepted: January 14, 2009

Abstract

Interstitial cells of Cajal (ICCs) have been identified as pacemaker cells in the upper urinary tract and urethra, but the role of ICCs in the bladder remains to be determined. We tested the hypotheses that ICCs express cyclooxygenase (COX), and that COX products (prostaglandins), are the cause of spontaneous rhythmic contraction (SRC) of isolated strips of rabbit bladder free of urothelium. SRC was abolished by 10 μM indomethacin and ibuprofen (non-selective COX inhibitors). SRC was concentration-dependently inhibited by selective COX-1 (SC-560 and FR-122047) and COX-2 inhibitors (NS-398 and LM-1685), and by SC-51089, a selective antagonist for the PGE-2 receptor (EP) and ICI-192,605 and SQ-29,548, selective antagonists for thromboxane receptors (TP). The partial agonist/antagonist of the PGF-2α receptor (FP), AL-8810, inhibited SRC by ~50%. Maximum inhibition was ~90% by SC-51089, ~80–85% by the COX inhibitors and ~70% by TP receptor antagonists. In the presence of ibuprofen to abolish SRC, PGE-2, sulprostone, misoprostol, PGF-2α and U-46619 (thromboxane mimetic) caused rhythmic contractions that mimicked SRC. Fluorescence immunohistochemistry coupled with confocal laser scanning microscopy revealed that c-Kit and vimentin co-localized to interstitial cells surrounding detrusor smooth muscle bundles, indicating the presence of extensive ICCs in rabbit bladder. Co-localization of COX-1 and vimentin, and COX-2 and vimentin by ICCs supports the hypothesis that ICCs were the predominant cell type in rabbit bladder expressing both COX isoforms. These data together suggest that ICCs appear to be an important source of prostaglandins that likely play a role in regulation of SRC. Additional studies on prostaglandin-dependent SRC may generate opportunities for the application of novel treatments for disorders leading to overactive bladder.

Keywords: ICC • COX-1 • COX-2 • prostaglandins • bladder • autonomous activity • rhythmic contraction • smooth muscle

Introduction

In experiments on Macacus monkey, cat and dog, Sherrington [1] demonstrated over a century ago that the bladder is not completely 'at rest' when neurogenic stimuli are absent. That is, detrusor smooth muscle (DSM) spontaneously contracts even during the filling phase, albeit, in a less coordinated fashion and with a significantly weaker amplitude than during voiding. Based on extensive whole animal denervation and *in vitro* whole bladder studies, Sherrington [1] wrote that, 'It seems therefore justifiable that...the rhythmic action of the monkey's bladder arises in its own muscular wall'. Although the function of spontaneous rhythmic contraction (SRC) remains unknown, Stewart [2] speculated in 1900 that '...such a type of activity [may enable] the bladder to adjust its size more easily to the ever increasing amount of its contents'. A more recent study using isolated DSM strips revealed that SRC is apparent in man, pig and rabbit, and that SRC is entirely atropine and tetrodotoxin insensitive [3].

[#] These authors contributed equally to this work.
*Correspondence to: Paul H. RATZ, Ph.D.,
Virginia Commonwealth University School of Medicine,
Departments of Biochemistry & Molecular Biology and Pediatrics,
1101 East Marshall Street, PO Box 980614,
Richmond, VA 23298–0614, USA.
E-mail: phratz@vcu.edu

doi:10.1111/j.1582-4934.2009.00714.x

Such activity can be identified in both isolated muscle strips [4] and intact bladder [5, 6]. Thus, SRC may be caused by mechanisms entirely intrinsic to DSM, and thus, may be myogenically derived [7–9].

Alternatively, another cell type within the bladder interstitium may be integral to regulation or generation of SRC. Interstitial cells of Cajal (ICCs) control contractile activity of gut smooth muscle [10], and a study by Smet *et al.* [11] was the first to identify ICCs in bladder. Recent studies support the notion that ICCs also reside in human, pig, rat, mouse and guinea-pig bladder interstitium [11–16] and rabbit urethra [17]. However, in the female WBB6F1 mouse, ICCs are reported to be restricted to the proximal ureter and absent from the bladder [18]. ICCs can form gap junctions with smooth muscle [19], and juxtracrine chemical synapses have been shown to form between ICCs and immune cells in rat bladder and other organs [13]. Lagou *et al.* [16] have proposed that ICCs of the mouse bladder wall outer muscle layer generate and modulate muscarinic receptor-stimulated phasic activity. De Jongh *et al.* [20] have proposed that distinct complex mechanisms likely involving urothelium, cyclooxygenase (COX) activity, ICCs and prostaglandins, regulate outer and inner muscle layers of the guinea-pig bladder. Thus, although bladder ICCs are proposed to participate in regulation of contraction, the precise role(s) of bladder ICCs remains to be determined [21].

We confirmed that SRC of isolated rabbit bladder strips free from underlying urothelium is not dependent on muscarinic receptor activation, and determined that SRC can be directly modulated by a non-genomic effect of sex steroids and relaxed by inhibitors of rhoA kinase but not by an inhibitor of conventional protein kinase C [22, 23]. Moreover, we showed that the average amplitude of SRC and the corresponding level of myosin light chain phosphorylation are greater in regions of the bladder closer to the dome than the trigone. SRC in isolated bladder strips appears to represent the activity of small functional units, termed autonomous modules [24]. In their work on autonomous activity, Drake *et al.* [6] proposed that '...in the bladder, ICCs and the intramural nerve plexus may have similar pacemaker and integrative functions [to ICCs and intramural nerves in the gut] and form the basis for initiating and coordinating non-micturating bladder activity'. The significance of this concept is that the intensity of SRC is age dependent [25] and patients exhibiting symptoms of overactive bladder display enhanced SRC and elevated numbers of ICCs [26]. Thus, although much has been discovered about SRC, one basic mechanistic question that remains to be answered is precisely how SRC is regulated.

Prostaglandins participate in regulation of smooth muscle contraction of several organ systems, including the vasculature, gut, airways and myometrium [27]. Early studies showed that prostaglandins are released into the circulation upon bladder stretch [28], and that prostaglandins participate in causing basal tone of bladder muscle in rabbit, rat, cat, dog, sheep and human but not guinea-pig [29]. However, the bladder cell type responsible for prostaglandin production and the precise role of prostaglandins in the regulation of bladder contractions, remain to be fully determined [30]. Phasic activity of guinea pig bladder appears to be regulated by prostaglandins [20], and very recent work from Gillespie's laboratory [31] supports the view that COX-1 is highly localized in guinea-pig bladder to urothelium and ICCs within the inner and not outer smooth muscle layer. We have found that, in the rabbit, SRC occurs in the absence of urothelium [22]. Thus, the present study was designed to test the hypotheses that, in isolated strips of rabbit bladder free of underlying urothelium, (*i*) prostaglandins play an essential role in regulating SRC and (*ii*) ICCs express COX, an enzyme responsible for prostaglandin production.

Materials and methods

Tissue preparation

Tissues were prepared as described previously [32, 33]. Whole bladders from adult female New Zealand white rabbits were removed immediately after killing with pentobarbital. Bladders were washed several times, cleaned of adhering tissue, including fat and serosa and stored in cold (0–4°C) physiologic salt solution (PSS), composed of NaCl, 140 mM; KCl, 4.7 mM; $MgSO_4$, 1.2 mM; $CaCl_2$, 1.6 mM; Na_2HPO_4, 1.2 mM; morpholinopropanesulfonic acid, 2.0 mM (adjusted to pH 7.4 at either 0 or 37°C, as appropriate); Na_2 ethylenediamine tetraacetic acid (to chelate trace heavy metals), 0.02; and dextrose, 5.6 mM. High purity (17 MΩ) water was used throughout. Longitudinal detrusor muscle strips free of underlying urothelium were cut from the wall of the bladder above the trigone. Thin muscle strips (~0.2 mm wide by ~1 cm long) were cut following the natural bundling that is clearly demarcated when bladders are in ice-cold buffer, as described previously [22]. Muscle tissues were incubated in aerated PSS at 37°C in water-jacketed tissue baths (Radnoti Glass Technology, Inc., Monrovia, CA, USA). Tissues that were to be stretched to their optimum length for muscle contraction (L_0) were secured by small clips to a micrometer for length adjustments and a tension transducer (Harvard Bioscience, Holliston, MA, USA; Radnoti Glass Technology, Inc.) for measurement of isometric contraction.

Contraction of isolated detrusor strips

Isometric contraction was measured as described previously [32, 34]. Voltage signals were digitized (model DIO-DAS16, ComputerBoards, Mansfield, MA, USA), visualized on a computer screen and stored for analyses. All data analyses were performed with a multichannel data integration program (DASYLab, DasyTec USA, Amherst, NH, USA). Tissues were equilibrated for a minimum of 30 min. suspended without tension between micrometer and tension transducer, then stretched to their optimum length for muscle contraction (L_0) using an abbreviated length-tension determination in which the optimum tension for muscle contraction (T_0) produced by 110 mM KCl at L_0 was obtained [35–37], and taking into consideration that contractions at short muscle lengths induced additional 'passive' tension that was eliminated by strain softening [38, 39]. To reduce tissue-to-tissue variability, subsequent contractions were reported as normalized to T_0 (T/T_0), or to the pre-antagonist value, T_i (see next section).

Concentration-response curves (CRCs)

To construct CRCs for the effects of specific COX and prostaglandin receptor antagonists on SRC, each antagonist was added to tissues in half-log increments starting with at least 10^{-10} M and ending with at most, 10^{-5} M, and tension was recorded for 10 min. After the 10-min. period following addition of the final concentration of antagonist, the tissue bath was drained and a Ca^{2+}-free solution was used to determine the minimum tension. The average tension and cycle frequency produced during a 2-min. interval prior to addition of each incremental concentration of receptor antagonist was recorded and normalized to the pre-antagonist value (T_i) and the final minimum value produced by incubation in the Ca^{2+}-free solution. The control tissues did not receive drug, but did receive dimethylsulfoxide (DMSO), the vehicle for most drugs used. To examine the contractile effects of prostaglandin agonists, SRC was abolished by addition of 10 μM ibuprofen, and a cumulative CRC for each given prostaglandin agonist was constructed by adding the stimulus to tissues in half-log increments starting with 10^{-8} M and ending with 3×10^{-6} M, and tension was recorded for about 10 min. The average tension and cycle frequency produced during a 2-min. interval prior to addition of each incremental concentration of receptor antagonist was recorded.

Fluorescence immunohistochemistry (FIHC) and confocal laser scanning microscopy

Tissues were prepared for FIHC by methods described previously [40] with some modifications. Bladder sheets were quickly frozen in liquid nitrogen-cooled isopentane and stored at –80°C for later processing, or immediately sectioned by cryostat to 8 μm and placed on a glass slide, fixed in 2% paraformaldehyde in phosphate-buffered saline (PBS) plus 0.1% Tween (PBS-T) for 10 min., permeabilized in 0.5% Triton X-100 in PBS-T for 30 min., and blocked in 10% Bovine serum albumin (BSA) in PBS-T for 1 hr. Tissue sections were dual-labelled with antibodies to vimentin (Sigma Aldrich, St. Louis, MO, USA; mouse monoclonal) and c-Kit (Santa Cruz Biotechnology, Santa Cruz, CA, USA; goat polyclonal), vimentin and COX-1 (Santa Cruz Biotechnology; goat polyclonal), vimentin and COX-2 (Santa Cruz Biotechnology; goat polyclonal), c-Kit and COX-1 and c-Kit and COX2, then dual-stained with DAPI (to identify nuclei) and phalloidin (to identify the actin-rich DSM cells). An example of a typical sequence of labelling and staining of tissues is as follows. Anti-COX-1 (1:10) or anti-COX-2 (1:10) antibody was applied overnight at 4°C, and the secondary antibody (Alexa Fluor 488 donkey anti-goat, Invitrogen; Carlsbad CA, USA) was applied at 1:500 for 1 hr at room temperature the following day. Anti-vimentin (1:100) or anti-c-kit (1:10) antibody was then applied for 1 hr at room temperature, and the secondary (Alexa Fluor 568 goat antimouse, Invitrogen) was applied at 1:500 for 1 hr at room temperature. Cytosolic actin was counterstained with phalloidin Alexa Fluor 647 (Invitrogen) at 1:40 in PBS-T plus 0.1% BSA for 10 min., and the nucleus was counterstained with 1μM DAPI (EMD Biosciences; San Diego, CA, USA) in PBS-T plus 0.1% BSA for 1 min. VectaShield (Vector Laboratories, Burlingame, CA, USA) was applied to reduce photobleaching. As an additional control, specificity of COX-1 and COX-2 was demonstrated by co-staining for COX-1 and COX-2 as described above in the presence of blocking peptides (COX-1 BP and COX-2 BP, Santa Cruz Biotechnology).

To ensure distinct separation of fluorescent signals, a Leica SP2 AOBS (Leica Microsystems Inc., Bannockburn, MI, USA) confocal laser scanning microscope was used, employing a combination of sequential and simultaneous scanning. For this, two sequential scans of spectrally distant pairs were performed (*i.e.* blue and red channels were scanned simultaneously followed by simultaneous scanning of green and far red channels). For each pair of fluors, the tunable liquid crystal filter (AOTF) was set to ensure that no cross-talk existed between the spectrally distant channels. For excitation, the following lasers were used: 450 nm diode (DAPI), 594 nm HeNe (Alexa Fluor 568), Argon 488 nm line (Alexa Fluor 488) and a 633 nm HeNe (Alexa Fluor 647). The SP detector windows were set to the following widths: 431–466 nm (DAPI), 607–642 nm (Alexa Fluor 568), 500–535 nm (Alexa Fluor 488) and 650–772 nm (Alexa Fluor 633).

Drugs and statistics

NS-398, SC-560, FR-122047, SQ-29,548, AL-8810, PGE-2, sulprostone, misoprostol and U-46619 were from Cayman Chemical (Annarbor, MI, USA). Indomethacin and PGF-2α were from Sigma. LM-1685 was from EMD Biosciences. ICI-192,605 and SC-51089 were from Biomol (Enzo Life Sciences International, Plymouth Meetings, PA, USA). All drugs were dissolved in de-ionized water or DMSO, and the latter was added at a final concentration no greater than 0.1%, a concentration that previously had shown, on average, no effect on SRC over a 40-min. time period [22]. Analysis of variance and the Student–Newman–Keuls test, or the t-test, were used where appropriate to determine significance, and the Null hypothesis was rejected at $P < 0.05$. The population sample size (n value) refers to the number of bladders, not the number of tissues.

Results

Effect of COX inhibitors on SRC

Tissues at L_0 were allowed to develop SRC for approximately 10 min., 10 μM indomethacin was added, and the degree of change in SRC was evaluated. Indomethacin completely abolished SRC (Fig. 1) and therefore reduced the frequency of spontaneous contractions to zero (compare Fig. 1D and E). These results indicated that SRC was dependent on COX activity, but because indomethacin is nearly equally effective at inhibition of COX-1 and COX-2 [41], the data did not address which isozyme was responsible for generation of SRC.

To determine whether COX-2 activity played a role in SRC, tissues at L_0 that had developed SRC were challenged with COX-2 selective antagonists cumulatively to produce a CRC. The vehicle control, DMSO, and time caused a reduction of the average rhythmic contraction of less than 10% (Fig. 2C and D, open symbols). NS-398, a selective COX-2 inhibitor, induced a concentration-dependent inhibition of SRC with an apparent IC_{50} value of ~3×10^{-9} M (Fig. 2C, square symbols). LM-1685, a selective COX-2 inhibitor structurally distinct from NS-398, also inhibited SRC with a less potent apparent IC_{50} of ~1×10^{-7} M (Fig. 2C, diamonds).

To determine whether COX-1 played a role in SRC, tissues were exposed to two COX-1 inhibitors that, like the COX-2 inhibitors, are structurally distinct. Like the COX-2 inhibitors, both SC-560 and FR-122047 greatly reduced the average SRC (Fig. 2D) and displayed apparent IC_{50} values for inhibition of, respectively,

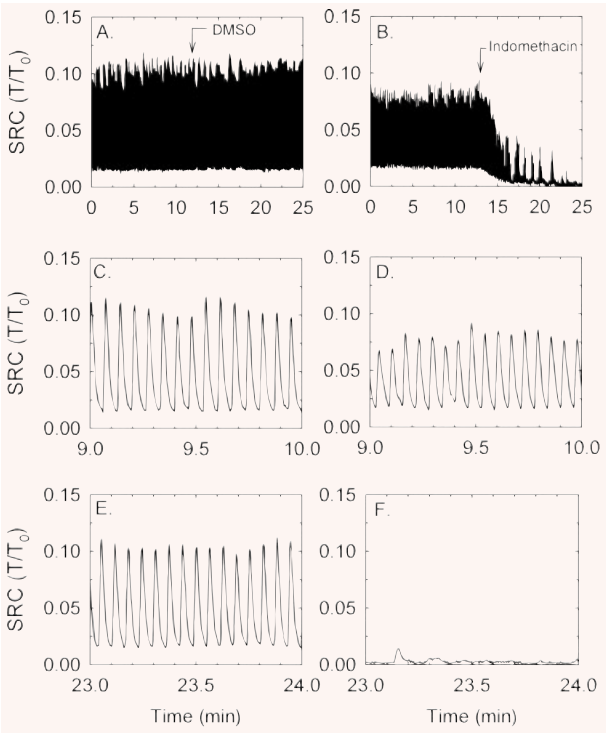

Fig 1. Example (from an $n = 3$ observations) of a temporal tension tracing showing that SRC is unaffected by ~10 min. of treatment with the vehicle control, 0.1% DMSO (**A**) and is abolished by 10 μM indomethacin (**B**). Expanded time scales of (**A**) and (**B**) reveal individual rhythmic contractions [(**C**) and (**E**) are time expanded from (**A**), and (**D**) and (**F**) are time expanded from **B**)] and the lack of effect of DMSO (**E**) and complete inhibition of SRC by indomethacin (**F**). Note that the *x*-axis time scales in the figure panels showing the time-expanded regions (**C–F**) refer to the time regions of plots (**A**) and (**B**) from which the data were extracted.

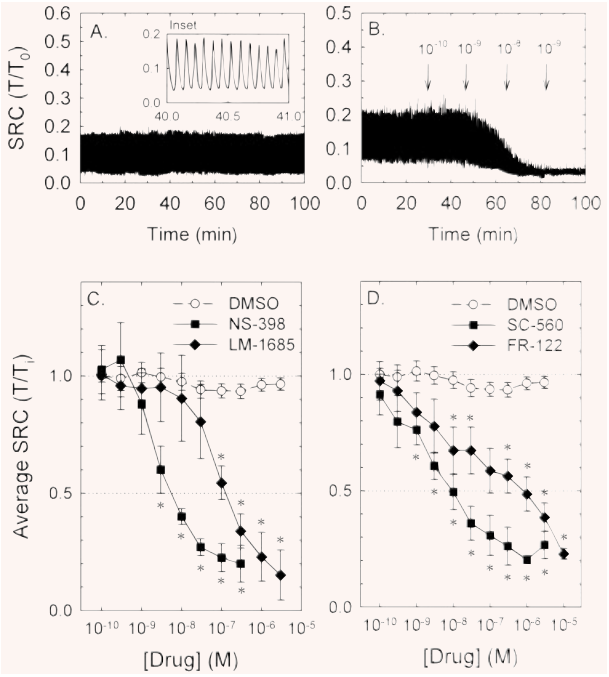

Fig 2. Compared to control, COX-1 and COX-2 inhibitors potently and efficaciously reduced SRC. Examples of a SRC that is maintained for 100 min. and unaffected by time and DMSO (**A**; expanded time scale of 'inset' reveals individual rhythmic contractions) and a SRC that is nearly abolished by the cumulative addition of increasing concentrations of the COX-2 inhibitor, NS-398 (**B**). Note that the *x*-axis time scale in the 'inset' of (**A**) shows the time-expanded region from which the data were extracted. Summary data for protocols shown in (**B**) for the COX-2 inhibitors, NS-398 and LM-1685 (**C**) and the COX-1 inhibitors, SC-560 and FR-122047 (FR-122) (**D**). Open symbols in (**C**) and (**D**) show the small average decline in SRC over time and in the presence of DMSO. Data in (**C**) and (**D**) are means ± S.E., $n = 4$–9. * = $P < 0.05$ compared to DMSO control.

~1×10^{-8} M and ~1×10^{-6} M. These data together suggest that both COX isozymes may participate in causing SRC.

Effect of prostaglandin inhibitors on SRC

The finding that inhibition of tissue COX activity abolished SRC supports the hypothesis that one or more prostaglandins released by a cell type within the bladder wall directly acted on DSM receptors to activate contraction or to enhance pacemaker activity causing the generation of SRC. Three candidate prostaglandins would include PGE-2, PGF-2α and thromboxane because these autacoids can activate G protein-coupled receptors linked to Gq or Gi/o that could theoretically cause DSM contraction. To determine which prostaglandin may have been responsible for inducing SRC, tissues were challenged with the PGE-2 receptor (EP1/3) antagonist, SC-51089, two thromboxane receptor (TP) antagonists, ICI-192,605 and SQ-29,548 and the PGF-2α receptor (FP) partial agonist and competitive antagonist, AL-8810. The EP1/3 antagonist concentration-dependently inhibited SRC (Fig. 3A, squares) with a high apparent potency (IC_{50} ~3×10^{-8} M) and maximum efficacy (~90%). The FP partial agonist/antagonist, AL-8810, inhibited SRC by ~50% at low concentrations and at concentrations greater than 3×10^{-7} M, lost its inhibitory effect and appeared to potentiate SRC (Fig. 3A, diamonds). Both TP antagonists produced a modest inhibition of SRC (Fig. 3B). Together, these data support the hypothesis that PGE-2, PGF-2α and thromboxane may all participate in inducing SRC, and suggest that PGE-2 may exert the greatest contribution.

Ability of prostaglandins to cause rhythmic contraction

If prostaglandins produced within the bladder wall were responsible for induction of SRC, then addition of exogenous prostaglandins

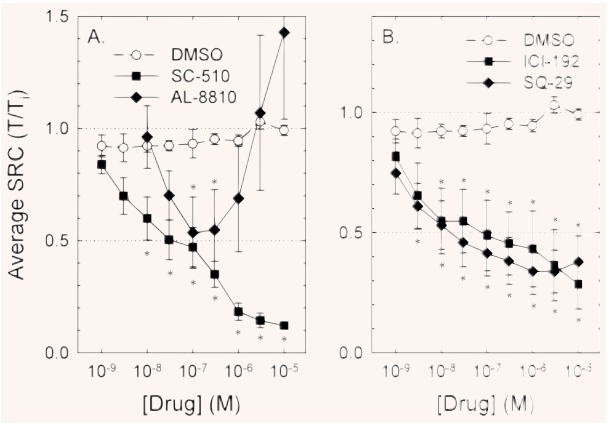

Fig 3. Compared to control (DMSO), the EP receptor antagonist, SC-51089 (**A**, SC-510) and the TP receptor antagonists, ICI-192,605 and SQ-29,548 (**B**, ICI-192 and SQ-29) produced concentration-dependent inhibition of SRC. The FP receptor partial agonist/antagonist, AL-8810, produced a biphasic response, causing ~50% inhibited SRC at 10^{-7} M (**A**). Data are means ± S.E., $n = 4$–9. * = $P < 0.05$ compared to DMSO control.

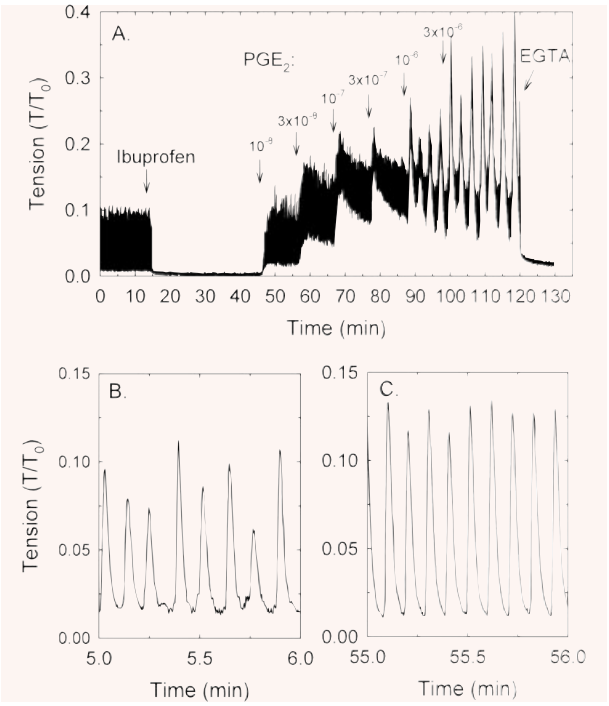

Fig 4. Example (of $n = 4$ observation) of the protocol used to measure the contractile effect of exogenously added prostaglandins (PGE-2 shown) after inhibition of SRC using 10 μM ibuprofen (**A**). EGTA was added at the end of the experiment to measure the minimum tension. Examples of SRC (**B**) and PGE-2-induced rhythmic contraction (**C**) shown in a time-expanded scale reveals the similar nature of the responses. Note that the *x*-axis time scales in the time-expanded regions (**B** and **C**) refer to the time regions of plot A from which the data were extracted.

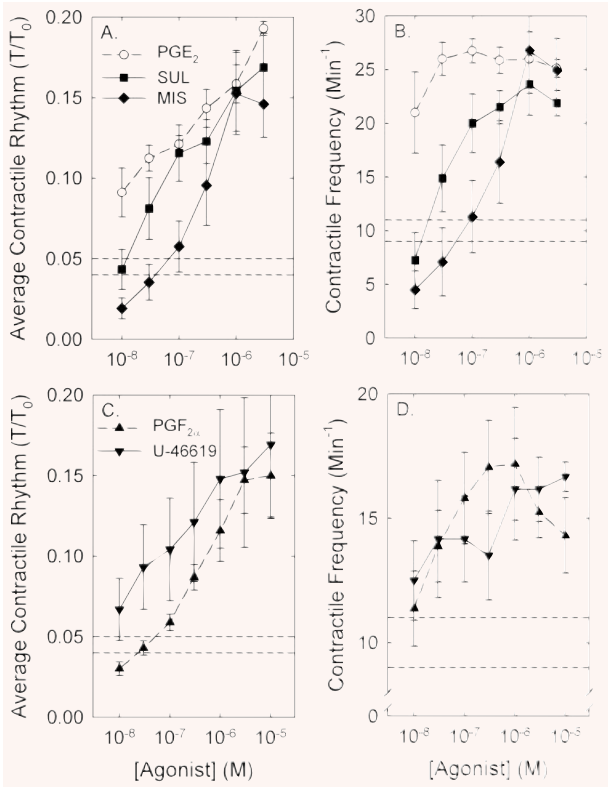

Fig 5. The average amplitudes (**A** and **C**) and frequencies (**B** and **D**) of rhythmic contractions produced by PGE-2 and the PGE-2-mimetics, sulprostone (SUL) and misoprostol (MIS; **A** and **B**) and PGF-2α and the thromboxane mimetic, U-46619 (**C** and **D**). For a comparison, the average plus S.E. and average minus S.E. values of control SRC are shown by dashed lines. Data are means ± S.E., $n = 4$–8.

should produce a contraction. To test this hypothesis, tissues were treated with 10 μM ibuprofen to abolish endogenous prostaglandin production and SRC, and challenged with PGE-2 and the EP 1/3 agonists, sulprostone and misoprostol. Each agonist was added individually to produce a cumulative CRC (see Fig. 4A). Ibuprofen, like indomethacin, abolished SRC, and all three agents caused modest contractions (see Fig. 4 for the effect of PGE-2). Notably, the form of contraction was rhythmic, despite the fact that tissues were exposed to constant (not varying) concentrations of PGE-2. Moreover, at a certain prostaglandin concentration, the rhythmic contraction was similar in amplitude and frequency to that induced spontaneously (*i.e.* similar to SRC; see Fig. 5). At concentrations greater than 10^{-6} M, contractions displayed a slower wave, higher amplitude rhythm (see Fig. 4A). PGE-2 induced the most potent contractile response compared to sulprostone and misoprostol (Fig. 5), and 10^{-8} M PGE-2 caused contraction that displayed an average tension value and a rhythmic frequency ~2-fold greater than that induced spontaneously (Fig. 5A and B, compare the open symbols at 10^{-8} M to the two horizontal dashed lines that represent the average plus S.E. and average minus S.E. values of the

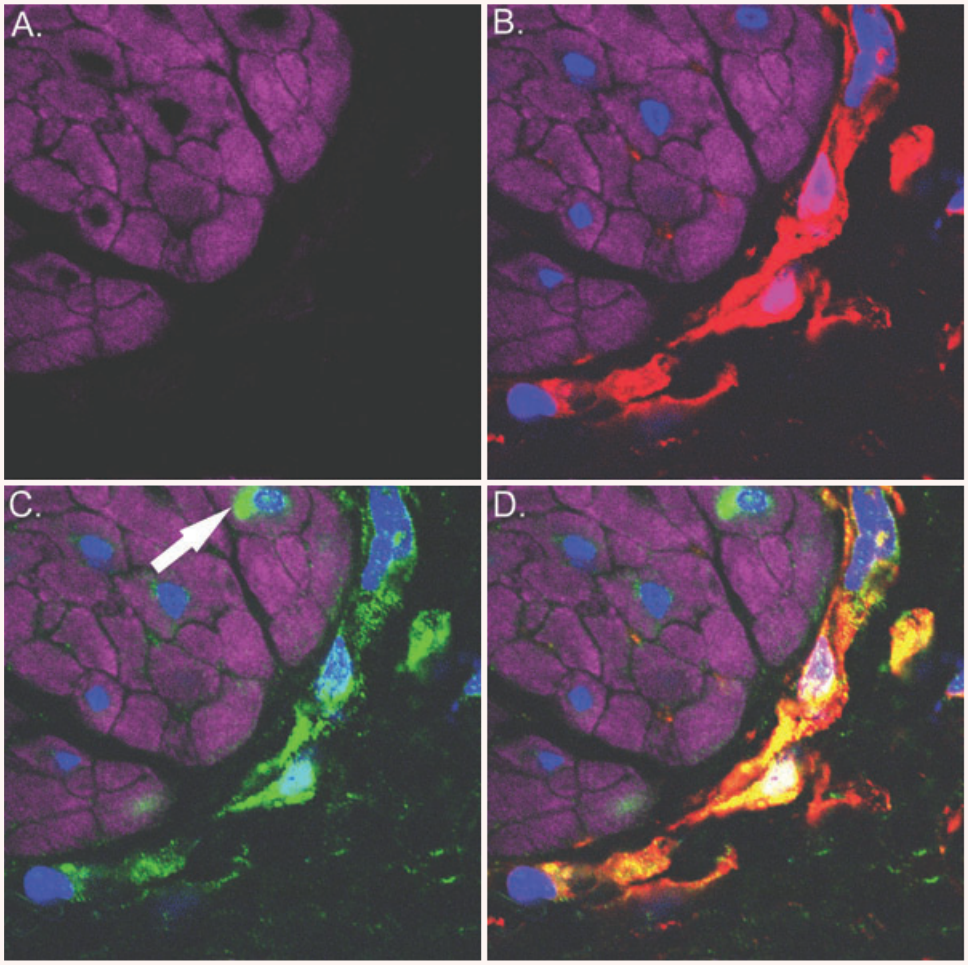

Fig 6. Scanning confocal microscopic images of rabbit bladder sections processed using FIHC reveal ICCs surrounding bundles of DSM. In all panels, purple staining (phalloidin) demonstrates DSM bundles, blue staining (DAPI) demonstrates nuclei and red staining (vimentin) or green staining (c-kit) demonstrates ICCs. (**A**) Image in which staining for vimentin and c-kit is withheld as a control revealing DSM bundles. (**B**) Identical image in which vimentin (red) identifies ICCs. (**C**) Identical image in which c-kit (green) identifies ICCs and was also identified surrounding the nuclei of some DSM cells (arrow). (**D**) Overlay image of (**B**) and (**C**) in which yellow staining reveals co-localization of vimentin and c-Kit on interstitial cells, supporting the hypothesis that interstitial cells in rabbit bladder are ICCs. This is a representative picture from $n = 3$ bladders.

control SRC). The maximum strength of contraction was ~0.15–0.2-fold that induced by KCl (*i.e.* modest in strength), and the maximum frequency achieved was ~25 cycles per min (Fig. 5). PGF-2α and the thromboxane mimetic, U-46619, likewise caused modest concentration-dependent rhythmic contractions, although the maximum frequency was less than that produced by the EP receptor agonists (Fig. 5C and D).

Location of COX-2 and COX-1 using FIHC laser scanning confocal microscopic analysis

Prostaglandins may have been produced by DSM or other cell types located within the bladder wall. ICCs have been identified in human, pig, rat, mouse and guinea-pig bladders. To determine whether ICCs reside in rabbit bladder, tissues processed for FIHC were labelled with antibodies to two proteins considered 'markers' for ICCs, vimentin and c-Kit [11, 12, 17, 42]. Although vimentin is expressed by fibroblasts and c-Kit is expressed by mast cells, c-Kit is not, and vimentin is only weakly expressed by DSM, and c-Kit receptors are not found on nerves and fibroblasts [43]. Thus, cells that express both vimentin and c-Kit can be identified as ICCs, and vimentin localization alone can serve as a useful probe to identify potential ICCs, especially because not all ICCs express c-kit [17, 31]. Tissues also were stained with fluorescently labelled DAPI and phalloidin to identify, respectively, nuclei and actin-rich DSM.

In tissue sections labelled with DAPI and phalloidin and then dual-labelled with vimentin and c-Kit, vimentin-positive (red) and

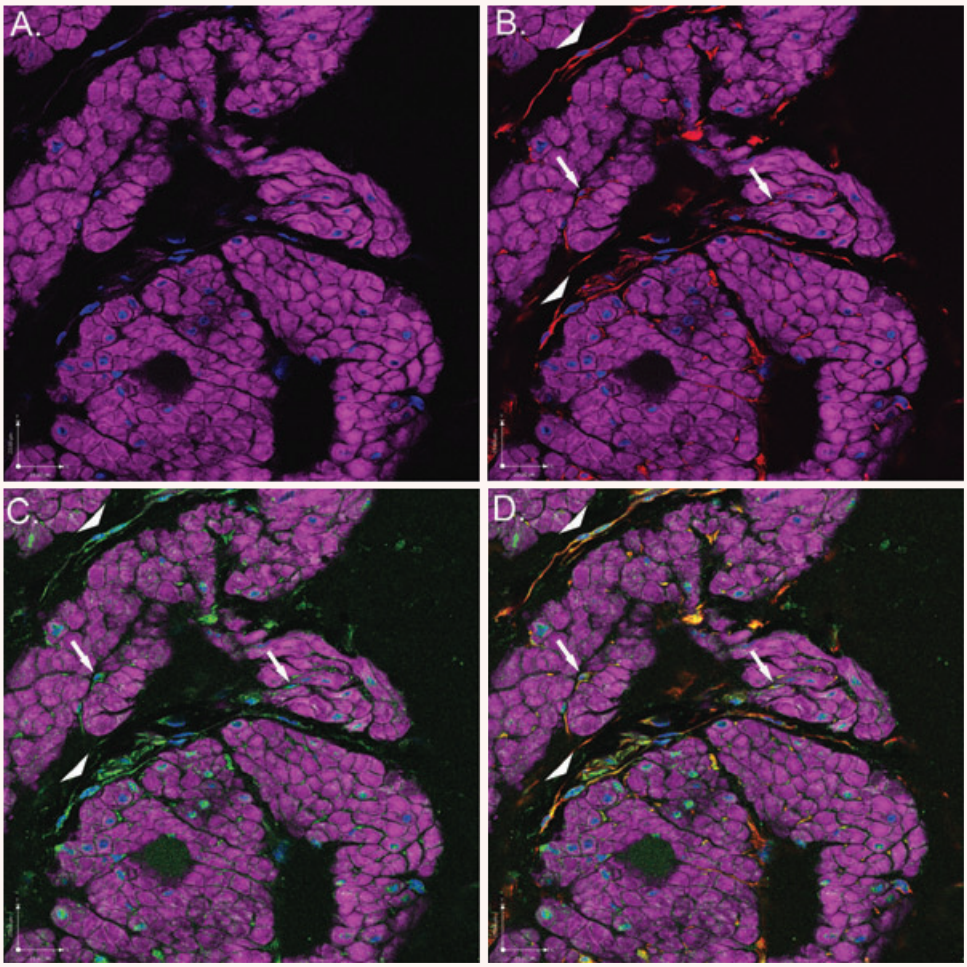

Fig 7. Scanning confocal microscopic images of rabbit bladder sections processed using FIHC reveal ICCs surrounding and within bundles of DSM. In all panels, purple staining (phalloidin) demonstrates DSM bundles, blue staining (DAPI) demonstrates nuclei and red staining (vimentin) or green staining (c-kit) demonstrates ICCs. (**A**) Image in which staining for vimentin and c-kit is withheld as a control revealing DSM bundles. (**B**) Identical image in which vimentin (red) identifies ICCs within (arrows) and surrounding (arrow heads) DSM bundles. (**C**) Identical image in which c-kit (green) identifies ICCs within (arrows) and surrounding (arrow heads) DSM bundles. (**D**) Overlay image of (**B**) and (**C**) in which yellow staining reveals co-localization of vimentin and c-Kit on interstitial cells within (arrows) and surrounding (arrow heads) DSM bundles, supporting the hypothesis that interstitial cells in rabbit bladder are ICCs. This is a representative picture from $n = 3$ bladders.

c-kit-positive (green) cells were identified surrounding bundles of DSM (purple) at high magnification (Fig. 6B and C) and both surrounding and within smooth muscle bundles at lower magnification (Fig. 7B and C). Specifically, vimentin and c-Kit displayed strong co-localization within the interstitial cells surrounding DSM bundles (Figs. 6D and 7D), indicating that rabbit bladders are populated with ICCs. Interestingly, c-Kit also labelled portions of the nucleus of many DSM cells (Fig. 6C, arrow).

To determine whether COX-2 and COX-1 were expressed on DSM and ICCs, tissue sections were labelled with antibodies to COX-2 and COX-1. COX-2 displayed strong co-localization with vimentin (Fig. 8) and c-kit (Fig. 9), supporting the hypothesis that rabbit bladder ICCs constitutively express COX-2. Likewise, COX-1 also co-localized with vimentin (Fig. 10) and c-kit (Fig. 11). COX-1 appeared also to be expressed by DSM in a punctuate fashion, especially in the periphery of cells (Fig. 10C). To establish the specificity of the primary antibodies, tissue sections labelled with DAPI and phalloidin were stained with COX-1 or COX-2 in the absence or presence of specific BP. Near abolishment of staining in the presence of BP demonstrates primary antibody specificity (Fig. 12). In addition, to rule out the possibility of

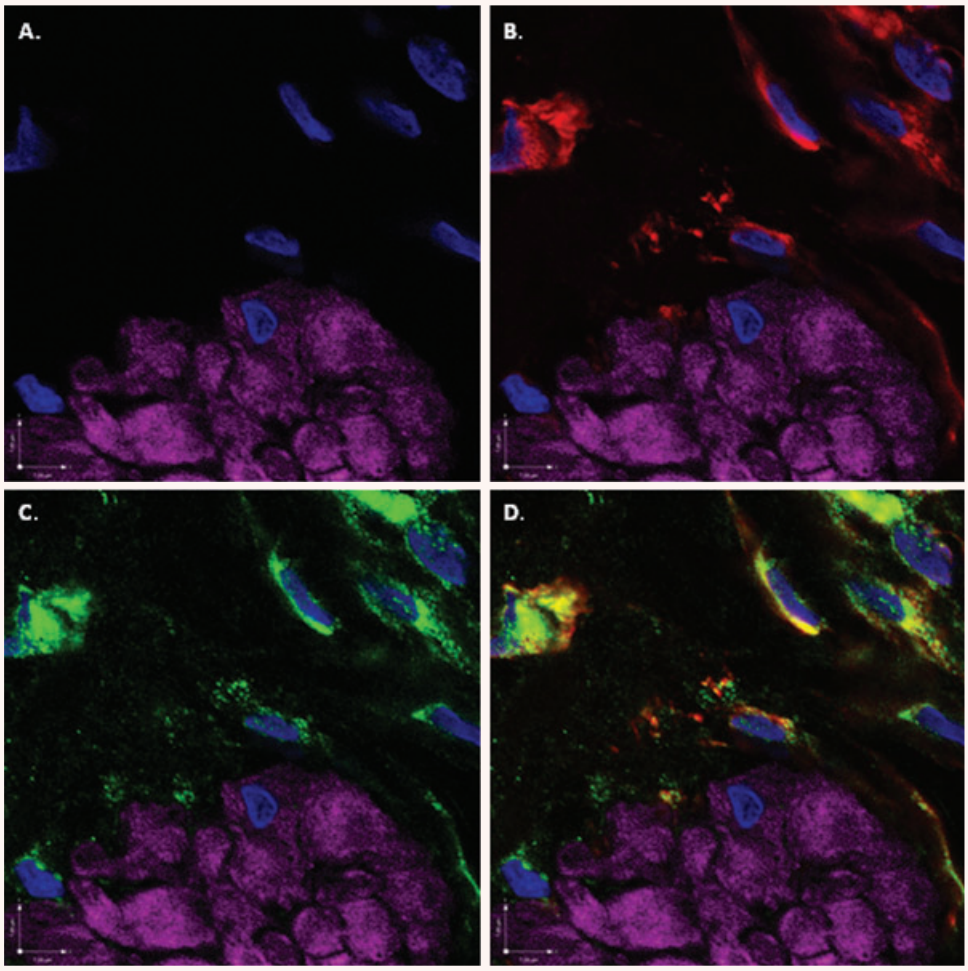

Fig 8. Scanning confocal microscopic images of rabbit bladder sections processed using FIHC reveal COX-2 expression in vimentin-positive ICCs surrounding DSM bundles. In all panels, purple staining (phalloidin) demonstrates DSM bundles and blue staining (DAPI) demonstrates nuclei. (**A**) Image in which staining for vimentin and COX-2 is withheld as a control revealing DSM bundles. (**B**) Identical image in which vimentin (green) identifies ICCs surrounding DSM bundles. (**C**) Identical image in which COX-2 (red) identifies ICCs surrounding DSM bundles. D. Overlay image of (**B**) and (**C**) in which yellow staining reveals co-localization of vimentin and COX-2 in ICCs. This is a representative picture from $n = 3$ bladders.

non-specific staining of the four secondary antibodies used as fluorophores, tissue sections labelled with DAPI and phalloidin were incubated only with secondary antibodies and there was no detectable non-specific tissue labelling (Fig. 13).

Discussion

Results from this study support a model in which ICCs participate in the regulation of SRC in rabbit bladder. In this model, ICCs constitutively express both COX-1 and COX-2, and we speculate that ICCs produce prostaglandins that participate in maintaining DSM SRC by acting on DSM prostaglandin receptors. These data support and extend the studies of Davidson and Lang [44] and Hashitani *et al.* [45] who showed that the spontaneous contractile activity of smooth muscles of the upper urinary tract and corpus cavernosum is dependent on endogenous prostaglandin production, and especially recent work by Gillespie's laboratory [20, 31] who show that epithelial cells within the urothelium, vimentin-positive cells that are likely ICCs in the lamina propria, and vimentin-negative cells in the lamina propria and inner muscle layer of guinea-pig bladder express COX-1. The major findings of our work are that rabbit bladder ICCs more so than DSM express COX-2 as well as COX-1, that bladder SRC can occur in tissues devoid of urothelium, and that SRC appears to be dependent on

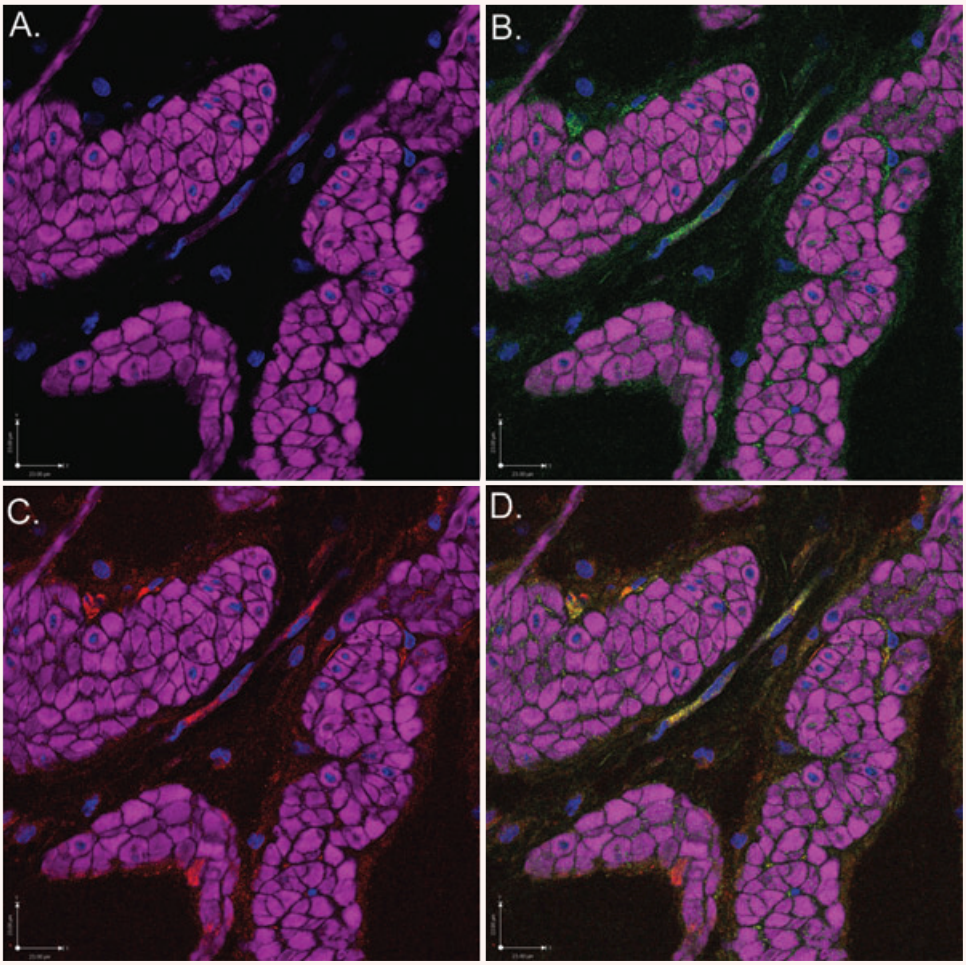

Fig 9. Scanning confocal microscopic images of rabbit bladder sections processed using FIHC reveal COX-2 expression in c-kit-positive ICCs surrounding DSM bundles. In all panels, purple staining (phalloidin) demonstrates DSM bundles and blue staining (DAPI) demonstrates nuclei. (**A**) Image in which staining for c-kit and COX-2 is withheld as a control revealing DSM bundles. (**B**) Identical image in which c-kit (green) identifies ICCs surrounding DSM bundles. (**C**) Identical image in which COX-2 (red) identifies ICCs surrounding DSM bundles. D. Overlay image of (**B**) and (**C**) in which yellow staining reveals co-localization of c-kit and COX-2 in ICCs. This is a representative picture from $n = 3$ bladders.

prostaglandins produced by COX. Thus, our data suggest that one function of bladder ICCs is to regulate the contractile state of DSM by bathing DSM bundles with a basal level of contractile prostaglandin. However, even though ICCs demonstrated greater immunoreactivity to COX antibodies than did DSM, we cannot rule out the possibility that DSM cells may also release substantial amounts of prostaglandins because of the vastly greater number of DSM cells than ICCs.

The rhythmic nature of tissue contractions requires that individual cell contractions become synchronized in time. ICCs in the outer muscle layers of the mouse bladder have been proposed to regulate phasic contractile activity [16], whereas in the guinea-pig, ICCs within the urothelium and inner muscle layer may play a role [20, 31]. The present study focused attention on ICCs surrounding muscle bundles in rabbit detrusor in which the urothelium was removed, and whether or not rabbit bladder expresses multiple ICC types was not investigated. Moreover, we did not exhaustively search for the tissue locations of all vimentin- and c-kit-positive cells. The precise nature of coordinated contraction remains somewhat elusive, because, although DSM cells are electrically coupled in the muscle bundle periphery [46], the extent of coupling is poor compared to 'classic' unitary smooth muscles such as that found in the gastrointestinal tract [47, 48]. However, DSM cells respond to rapid muscle stretch with a rapid and transient

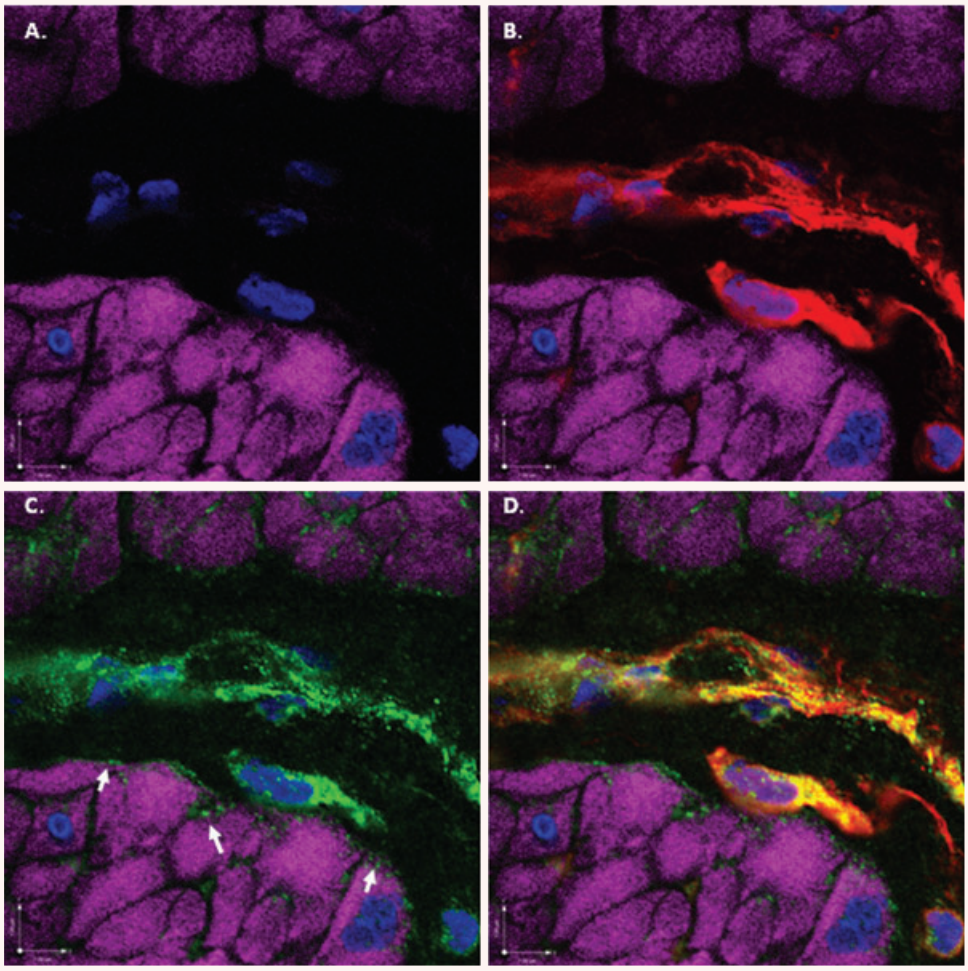

Fig 10. Scanning confocal microscopic images of rabbit bladder sections processed using FIHC reveal COX-1 expression in vimentin-positive ICCs surrounding DSM bundles. In all panels, purple staining (phalloidin) demonstrates DSM bundles and blue staining (DAPI) demonstrates nuclei. (**A**) Image in which staining for vimentin and COX-1 is withheld as a control revealing DSM bundles. (**B**) Identical image in which vimentin (green) identifies ICCs surrounding DSM bundles. (**C**) Identical image in which COX-1 (red) identifies ICCs surrounding DSM bundles. D. Overlay image of (**B**) and (**C**) in which yellow staining reveals co-localization of vimentin and COX-1 in ICCs. This is a representative picture from $n = 3$ bladders.

(short-lived) contraction termed the 'myogenic response' [49, 50]. That is, like arterioles and many other smooth muscle tissues [51], in response to straining cells by mechanically 'pulling' them or subjecting them to a hypo-osmotic solution, DSM cells depolarize [52] and transiently contract [49, 53]. Thus, although speculative, we propose a model in which prostaglandins released from ICCs surrounding muscle bundles induce rapid contraction of a population of electrically coupled DSM cells located in the muscle bundle periphery. This rapid coordinated contraction stretches adjacent DSM cells within muscle bundles leading to membrane depolarization of the stretched cells, causing a myogenic response within the muscle bundle. The net result is a coordinated muscle bundle contraction resulting in SRC.

It is now generally accepted that ICCs act as electrical pacemaker cells and regulators of smooth muscle contraction in the gastrointestinal tract [10], and recent studies identify ICCs as pacemakers of the urethra [54] and ureters [55]. Although electrically coupled ICCs have been identified in the bladder wall [12, 56] and a role for ICCs in regulation of phasic activity has been proposed [16, 20], the precise role ICCs play in bladder contraction remains to be determined. If there is an intrinsic pacemaker, prostaglandins released by ICCs may enhance the

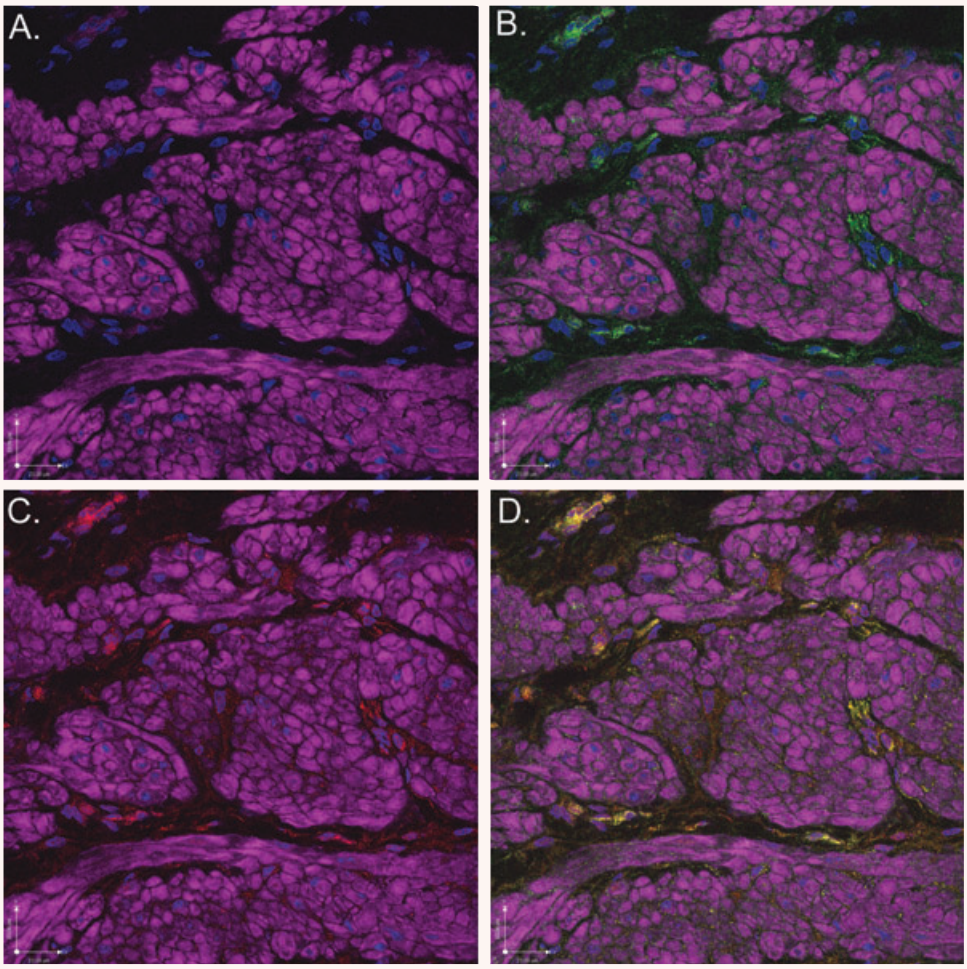

Fig 11. Scanning confocal microscopic images of rabbit bladder sections processed using FIHC reveal COX-1 expression in c-kit-positive ICCs surrounding DSM bundles. In all panels, purple staining (phalloidin) demonstrates DSM bundles and blue staining (DAPI) demonstrates nuclei. (**A**) Image in which staining for c-kit and COX-1 is withheld as a control revealing DSM bundles. (**B**) Identical image in which c-kit (green) identifies ICCs surrounding DSM bundles. (**C**) Identical image in which COX-1 (red) identifies ICCs surrounding DSM bundles. D. Overlay image of (**B**) and (**C**) in which yellow staining reveals co-localization of c-kit and COX-1 in ICCs. This is a representative picture from $n = 3$ bladders.

frequency of pacemaker activity. The present study is the first to show that rabbit bladder ICCs constitutively express both COX-1 and COX-2, and that selective COX-1 and COX-2 inhibition can exert a potent and highly efficacious inhibition of SRC. These results support and extend earlier reports that indomethacin and other non-selective COX inhibitors reduce SRC in bladder strips isolated from several mammalian species [29, 57]. The precise prostaglandin species responsible for initiating SRC was not determined in this study. However, our data support the notion that PGE-2 may play a prominent role because selective EP receptor inhibition nearly abolished SRC. PGF-2α and thromboxane may also participate because inhibition of, respectively, FP and TP receptors, reduced but did not abolish SRC. Moreover, addition of PGE-2 and its analogues, sulprostone and misoprostol, and PGF-2α and the thromboxane mimetic, U-46619, to tissues in which SRC was abolished by ibuprofen caused the initiation of rhythmic contractions similar in amplitude and frequency to SRC. Although COX-2 is expressed primarily during inflammation of tissues, COX-2 appears to be constitutively expressed by corpus cavernosum smooth muscle [45] and upper urinary smooth muscle of the guinea-pig but not rat, where COX-1 appears to play the predominant role [44]. Thus, these reports and our present findings support the hypothesis that COX-2 plays an integral role in constitutive

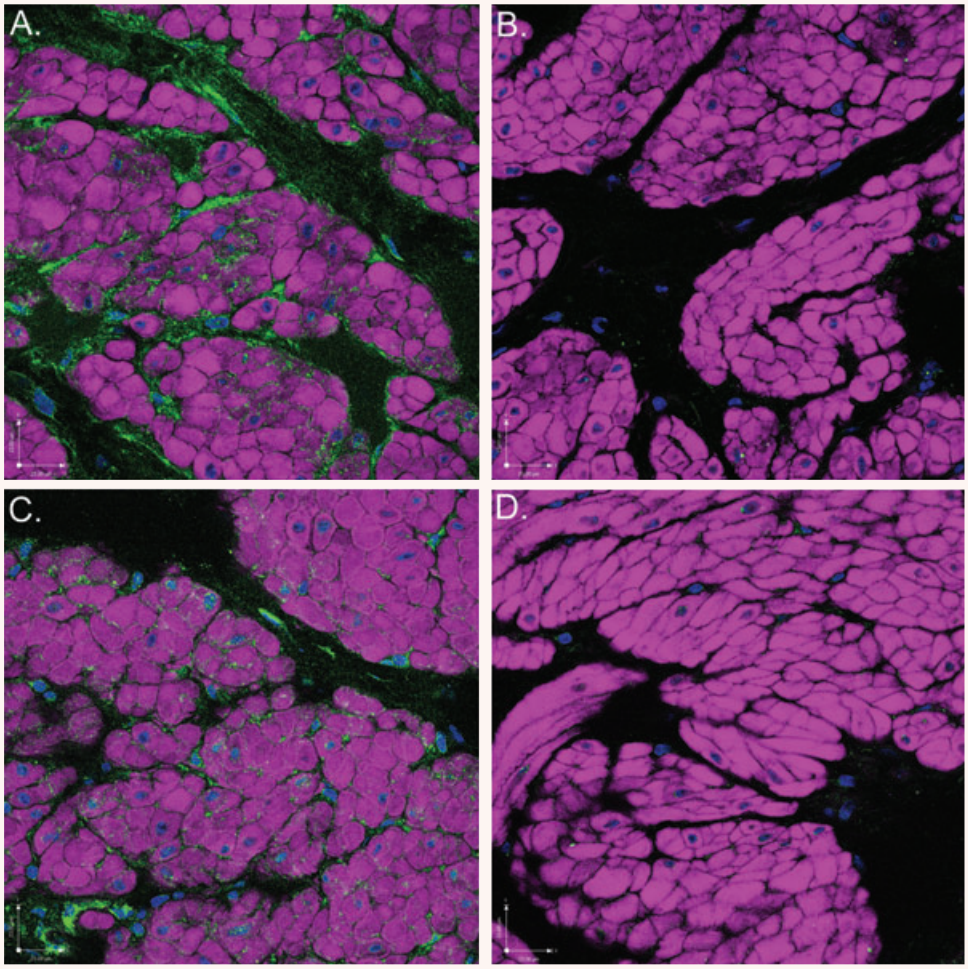

Fig 12. Scanning confocal microscopic images of rabbit bladder sections processed using FIHC indicate near abolishment of COX-2 and COX-1 staining in the presence of specific BP. All images are dual-stained with phalloidin (purple) to demonstrate DSM morphology and DAPI (blue) to demonstrate nuclear morphology. (**A**) COX-1 expression (green) on ICCs surrounding DSM bundles. (**B**) COX-1 expression is nearly abolished in the presence of COX-1 BP. (**C**) COX-2 expression (green) on ICCs surround DSM bundles. (**D**) COX-2 expression is nearly abolished in the presence of COX-2 BP.

prostaglandin production in the urogential tract of some mammalian species.

COX-1 and COX-2 expression and prostaglandin synthesis are increased during bladder obstruction, bladder distension, and in the chronically ischemic bladder [28, 58, 59], conditions that can lead to overactive bladder. In human beings and rat, PGE-2 causes destrusor overactivity, and in human beings, this is associated with decreased bladder capacity [60, 61]. In the spinal cord injury model of hyper-reflexic overactive bladder, there is an increase in PGE-2 release [62], and prostaglandins are proposed to participate in this C-fibre afferent nerve-regulated detrusor overactivity [63].

There is ample evidence in the basic science literature, demonstrating the effects of COX-inhibitors on micturition and/or bladder contractile activity in rats [64], rabbits [65], guinea-pigs [66] and cats [67]. However, clinical studies demonstrating efficacy of these agents in the treatment of voiding dysfunction are limited. Cardozo *et al.* [68] treated 30 women with detrusor instability with the NSAID, flurbiprofen, or placebo and demonstrated significant reductions in frequency, urgency and urge incontinence. Additionally, a study in paediatric patients after bladder surgery [69] demonstrated that the NSAID ketorolac reduced the frequency and severity of bladder spasms assessed by parental observation. On the other hand, Delaere [70] treated 55 patients with overactive bladder, refractory to available medical therapy with a 6-week course of indomethacin. Only a minority (17%) benefited from therapy, with side effects encountered in 42%. Likewise, Chaudhuri *et al.* [71] used radionucleotide imaging to

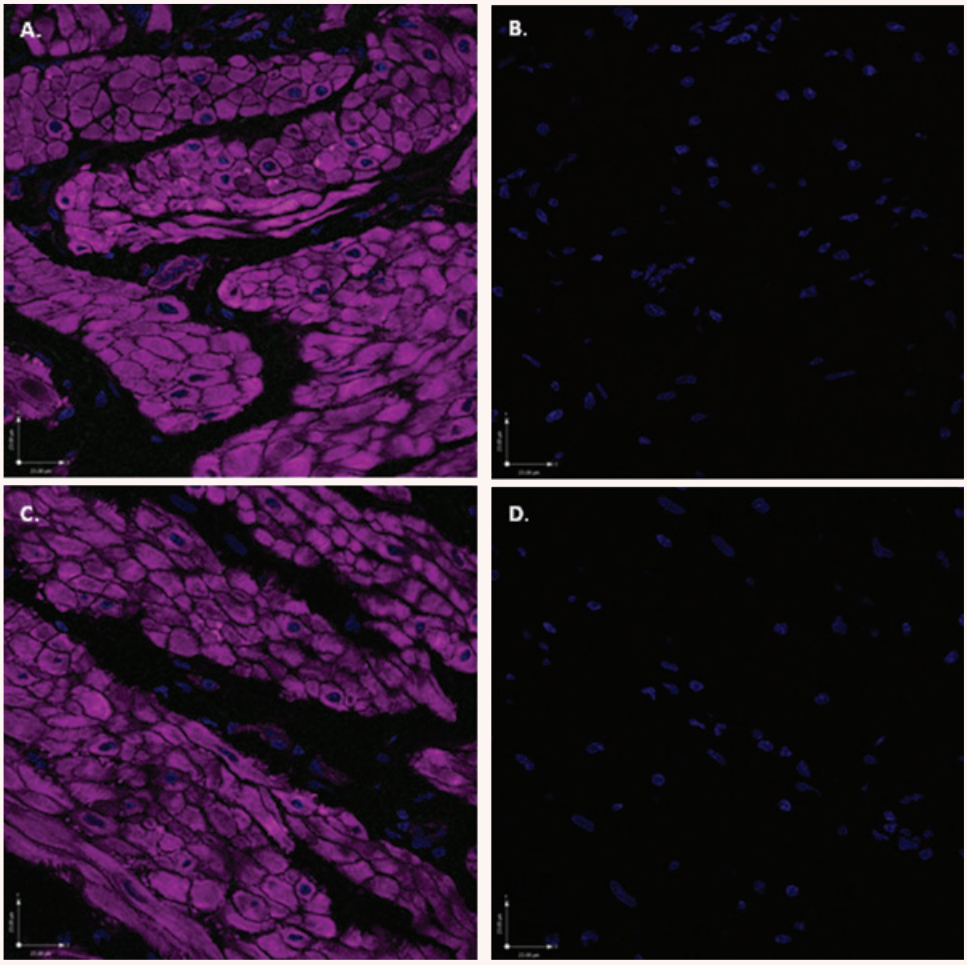

Fig 13. Scanning confocal microscopic images of rabbit bladder sections processed using FIHC indicate an absence of non-specific labelling with secondary antibodies. All images were labelled with phalloidin (purple) and DAPI (blue) and were exposed to the four excitation wavelengths described in the methods and corresponding to the colours blue (405 nm), green (488 nm), red (568 nm) and purple (647 nm). (**A**) Addition of secondary antibody Alexa Fluor 488 (without primary antibody) reveals no evidence of non-specific green staining. (**B**) In the identical image, digital subtraction of the purple colour does not uncover any subtle non-specific green staining in the region of the DSM bundles. (**C**) In an additional section labelled with phalloidin and DAPI, addition of the secondary antibody Alexa Fluor 568 (without primary antibody), reveals no evidence of non-specific red staining. (**D**) In the identical image, digital subtraction of the purple colour does not uncover any subtle non-specific red staining.

assess urodynamic parameters in 17 men treated with indomethacin or placebo and found no differences in any voiding parameters.

This information, along with results from the present study, suggests that a novel target for overactive bladder may be the selective inhibition of bladder ICC-induced production of prostaglandins.

Acknowledgements

The authors thank Vikram K. Sabarwal, Patrick C. Headley, Corey Johnson and Kenneth A. Ewane for their expert technical assistance. The authors acknowledge the support of the National Institutes of Health (R01-DK59620 to P.H.R) and Virginia Commonwealth University AD Williams grant (to A.P.K.).

References

1. **Sherrington CS.** Notes on the arrangement of some motor fibres in the lumbo-sacral plexus. *J Physiol*. 1892; 13: 621–772.
2. **Stewart CC.** Mammalian smooth muscles – the cat's bladder. *Am J Physiol*. 1900; 4: 185–208.
3. **Sibley GN.** A comparison of spontaneous and nerve-mediated activity in bladder muscle from man, pig and rabbit. *J Physiol*. 1984; 354: 431–43.
4. **Coolsaet BLRA, Blaivas JG.** No detrusor is stable. *Neurourol Urodyn*. 1985; 4: 259–61.
5. **Gillespie JI, Harvey IJ, Drake MJ.** Agonist- and nerve-induced phasic activity in the isolated whole bladder of the guinea pig: evidence for two types of bladder activity. *Exp Physiol*. 2003; 88: 343–57.
6. **Drake MJ, Harvey IJ, Gillespie JI.** Autonomous activity in the isolated guinea pig bladder. *Exp Physiol*. 2003; 88: 19–30.
7. **Brading AF.** A myogenic basis for the overactive bladder. *Urology*. 1997; 50: 57–67.
8. **Artibani W.** Diagnosis and significance of idiopathic overactive bladder. *Urology*. 1997; 50: 25–32.
9. **van Duyl WA, van der Hoeven AAM, de Bakker JV.** Synchronization of spontaneous contraction activity in smooth muscle of urinary bladder. *Neurourol Urodyn*. 1990; 9: 547–50.
10. **Sanders KM, Ward SM.** Interstitial cells of Cajal: a new perspective on smooth muscle function. *J Physiol*. 2006; 576: 721–6.
11. **Smet PJ, Jonavicius J, Marshall VR, *et al.*** Distribution of nitric oxide synthase-immunoreactive nerves and identification of the cellular targets of nitric oxide in guinea-pig and human urinary bladder by cGMP immunohistochemistry. *Neuroscience*. 1996; 71: 337–48.
12. **McCloskey KD, Gurney AM.** Kit positive cells in the guinea pig bladder. *J Urol*. 2002; 168: 832–6.
13. **Popescu LM, Gherghiceanu M, Cretoiu D, *et al.*** The connective connection: interstitial cells of Cajal (ICC) and ICC-like cells establish synapses with immunoreactive cells. Electron microscope study *in situ*. *J Cell Mol Med*. 2005; 9: 714–30.
14. **Metzger R, Neugebauer A, Rolle U, *et al.*** C-Kit receptor (CD117) in the porcine urinary tract. *Pediatr Surg Int*. 2008; 24: 67–76.
15. **Lagou M, De Vente J, Kirkwood TB, *et al.*** Location of interstitial cells and neurotransmitters in the mouse bladder. *BJU Int*. 2006; 97: 1332–7.
16. **Lagou M, Drake MJ, Markerink VANIM, *et al.*** Interstitial cells and phasic activity in the isolated mouse bladder. *BJU Int*. 2006; 98: 643–50.
17. **Sergeant GP, Hollywood MA, McCloskey KD, *et al.*** Specialised pacemaking cells in the rabbit urethra. *J Physiol (Lond)*. 2000; 526: 359–66.
18. **Pezzone MA, Watkins SC, Alber SM, *et al.*** Identification of c-kit-positive cells in the mouse ureter: the interstitial cells of Cajal of the urinary tract. *Am J Physiol Renal Physiol*. 2003; 284: F925–9.
19. **Takeda Y, Ward SM, Sanders KM, *et al.*** Effects of the gap junction blocker glycyrrhetinic acid on gastrointestinal smooth muscle cells. *Am J Physiol Gastrointest Liver Physiol*. 2005; 288: G832–41.
20. **de Jongh R, van Koeveringe GA, van Kerrebroeck PE, *et al.*** The effects of exogenous prostaglandins and the identification of constitutive cyclooxygenase I and II immunoreactivity in the normal guinea pig bladder. *BJU Int*. 2007; 100: 419–29.
21. **McHale NG, Hollywood MA, Sergeant GP, *et al.*** Organization and function of ICC in the urinary tract. *J Physiol*. 2006; 576: 689–94.
22. **Ratz PH, Miner AS.** Length-dependent regulation of basal myosin phosphorylation and force in detrusor smooth muscle. *Am J Physiol Regul Integr Comp Physiol*. 2003; 284: R1063–70.
23. **Shenfeld OZ, McCammon KA, Blackmore PF, *et al.*** Rapid effects of estrogen and progesterone on tone and spontaneous rhythmic contractions of the rabbit bladder. *Urol Res*. 1999; 27: 386–92.
24. **Drake MJ, Mills IW, Gillespie JI.** Model of peripheral autonomous modules and a myovesical plexus in normal and overactive bladder function. *Lancet*. 2001; 358: 401–3.
25. **Szigeti GP, Somogyi GT, Csernoch L, *et al.*** Age-dependence of the spontaneous activity of the rat urinary bladder. *J Muscle Res Cell Motil*. 2005; 26: 23–9.
26. **Brading AF, McCloskey KD.** Mechanisms of Disease: specialized interstitial cells of the urinary tract–an assessment of current knowledge. *Nat Clin Pract Urol*. 2005; 2: 546–54.
27. **Konturek SJ, Pawlik W.** Physiology and pharmacology of prostaglandins. *Dig Dis Sci*. 1986; 31: 6S–19S.
28. **Gilmore NJ, Vane JR.** Hormones released into the circulation when the urinary bladder of the anaesthetized dog is distended. *Clin Sci*. 1971; 41: 69–83.
29. **Hills NH.** Prostaglandins and tone in isolated strips of mammalian bladder [proceedings]. *Br J Pharmacol*. 1976; 57: 464P–5P.
30. **Andersson KE, Arner A.** Urinary bladder contraction and relaxation: physiology and pathophysiology. *Physiol Rev*. 2004; 84: 935–86.
31. **de Jongh R, Grol S, van Koeveringe G, *et al.*** The localisation of cyclo-oxygenase immuno-reactivity (COX I-IR) to the urothelium and to interstitial cells in the bladder wall. *J Cell Mol Med*. DOI: 10.1111/j.1582-2934.2008.00475.x.
32. **Shenfeld OZ, Morgan CW, Ratz PH.** Bethanechol activates a post-receptor negative feedback mechanism in rabbit urinary bladder smooth muscle. *J Urol*. 1998; 159: 252–7.
33. **Ratz PH.** High α_1-adrenergic receptor occupancy decreases relaxing potency of nifedipine by increasing myosin light chain phosphorylation. *Circ Res*. 1993; 72: 1308–16.
34. **Ratz PH.** Receptor activation induces short-term modulation of arterial contractions: memory in vascular smooth muscle. *Am J Physiol*. 1995; 269: C417–23.
35. **Uvelius B.** Isometric and isotonic length-tension relations and variations in longitudinal smooth muscle from rabbit urinary bladder. *Acta Physiol Scand*. 1976; 97: 1–12.
36. **Herlihy JT, Murphy RA.** Length-tension relationship of smooth muscle of the hog carotid artery. *Circ Res*. 1973; 33: 257–83.
37. **Ratz PH, Murphy RA.** Contributions of intracellular and extracellular Ca^{2+} pools to activation of myosin phosphorylation and stress in swine carotid media. *Circ Res*. 1987; 60: 410–21.
38. **Speich JE, Borgsmiller L, Call C, *et al.*** ROK-induced cross-link formation stiffens passive muscle: reversible strain-induced stress softening in rabbit detrusor. *Am J Physiol Cell Physiol*. 2005; 289: C12–21.
39. **Speich JE, Dosier C, Borgsmiller L, *et al.*** Adjustable passive length-tension curve in rabbit detrusor smooth muscle. *J Appl Physiol*. 2007; 102: 1746–55.
40. **Urban NH, Berg KM, Ratz PH.** K+ depolarization induces RhoA kinase translocation to caveolae and Ca2+ sensitization of

arterial muscle. *Am J Physiol Cell Physiol*. 2003; 285: C1377–85.

41. **Mitchell JA, Akarasereenont P, Thiemermann C, *et al.*** Selectivity of nonsteroidal antiinflammatory drugs as inhibitors of constitutive and inducible cyclooxygenase. *Proc Natl Acad Sci USA*. 1993; 90: 11693–7.
42. **Rumessen JJ, Thuneberg L.** Pacemaker cells in the gastrointestinal tract: interstitial cells of Cajal. *Scand J Gastroenterol Suppl*. 1996; 216: 82–94.
43. **Davidson RA, McCloskey KD.** Morphology and localization of interstitial cells in the guinea pig bladder: structural relationships with smooth muscle and neurons. *J Urol*. 2005; 173: 1385–90.
44. **Davidson ME, Lang RJ.** Effects of selective inhibitors of cyclo-oxygenase-1 (COX-1) and cyclo-oxygenase-2 (COX-2) on the spontaneous myogenic contractions in the upper urinary tract of the guinea-pig and rat. *Br J Pharmacol*. 2000; 129: 661–70.
45. **Hashitani H, Yanai Y, Shirasawa N, *et al.*** Interaction between spontaneous and neurally mediated regulation of smooth muscle tone in the rabbit corpus cavernosum. *J Physiol*. 2005; 569: 723–35.
46. **Hashitani H, Fukuta H, Takano H, *et al.*** Origin and propagation of spontaneous excitation in smooth muscle of the guinea-pig urinary bladder. *J Physiol*. 2001; 530: 273–86.
47. **Bramich NJ, Brading AF.** Electrical properties of smooth muscle in the guinea-pig urinary bladder. *J Physiol*. 1996; 492: 185–98.
48. **Hashitani H, Bramich NJ, Hirst GD.** Mechanisms of excitatory neuromuscular transmission in the guinea-pig urinary bladder. *J Physiol*. 2000; 524: 565–79.
49. **Burnstock G, Prosser CL.** Response of smooth muscles to quick stretch; relation of stretch to conduction. *Am J Physiol*. 1960; 198: 921–5.
50. **Poley RN, Dosier CR, Speich JE, *et al.*** Stimulated calcium entry and constitutive RhoA kinase activity cause stretch-induced detrusor contraction. *Eur J Pharmacol*. 2008; 599: 137–45.
51. **Johnson PC.** The myogenic response. In: David F, Bohr APS, Harvey V Sparks Jr, editors. Handbook of physiology: the cardiovascular system; vascular smooth muscle. Bethesda: American Physiological Society; 1980. pp. 409–42.
52. **Wellner C, Isenberg G.** Stretch effects on whole-cell currents of guinea-pig urinary bladder myocytes. *J Physiol*. 1994; 480: 439–48.
53. **Masters JG, Neal DE, Gillespie JI.** Contractions in human detrusor smooth muscle induced by hypo-osmolar solutions. *J Urol*. 1999; 162: 581–9.
54. **Sergeant GP, Hollywood MA, McHale NG, *et al.*** Ca2+ signalling in urethral interstitial cells of Cajal. *J Physiol*. 2006; 576: 715–20.
55. **Lang RJ, Tonta MA, Zoltkowski BZ, *et al.*** Pyeloureteric peristalsis: role of atypical smooth muscle cells and interstitial cells of Cajal-like cells as pacemakers. *J Physiol*. 2006; 576: 695–705.
56. **Sui GP, Rothery S, Dupont E, *et al.*** Gap junctions and connexin expression in human suburothelial interstitial cells. *BJU Int*. 2002; 90: 118–29.
57. **Anderson GF, Kohn KI.** Interactions of calcium, prostaglandins and indomethacin on the smooth muscle of the bladder. *Pharmacology*. 1978; 16: 306–13.
58. **Azadzoi KM, Shinde VM, Tarcan T, *et al.*** Increased leukotriene and prostaglandin release, and overactivity in the chronically ischemic bladder. *J Urol*. 2003; 169: 1885–91.
59. **Park JM, Yang T, Arend LJ, *et al.*** Obstruction stimulates COX-2 expression in bladder smooth muscle cells via increased mechanical stretch. *Am J Physiol*. 1999; 276: F129–36.
60. **Ishizuka O, Mattiasson A, Andersson KE.** Prostaglandin E2-induced bladder hyperactivity in normal, conscious rats: involvement of tachykinins? *J Urol*. 1995; 153: 2034–8.
61. **Schussler B.** Comparison of the mode of action of prostaglandin E2 (PGE2) and sulprostone, a PGE2-derivative, on the lower urinary tract in healthy women. A urodynamic study. *Urol Res*. 1990; 18: 349–52.
62. **Masunaga K, Yoshida M, Inadome A, *et al.*** Prostaglandin E2 release from isolated bladder strips in rats with spinal cord injury. *Int J Urol*. 2006; 13: 271–6.
63. **Maggi CA.** Prostanoids as local modulators of reflex micturition. *Pharmacol Res*. 1992; 25: 13–20.
64. **Angelico P, Guarneri L, Velasco C, *et al.*** Effect of cyclooxygenase inhibitors on the micturition reflex in rats: correlation with inhibition of cyclooxygenase isozymes. *BJU Int*. 2006; 97: 837–46.
65. **Bolle P, Tucci P.** Response to isoproterenol of rabbit detrusor strips following exposure to NSAIDs. *Pharmacol Res*. 1998; 37: 395–401.
66. **Doggrell SA, Scott GW.** The effects of time and indomethacin on contractile responses of the guinea-pig gall bladder *in vitro*. *Br J Pharmacol*. 1980; 71: 429–34.
67. **Wibberley A, McCafferty GP, Evans C, *et al.*** Dual, but not selective, COX-1 and COX-2 inhibitors, attenuate acetic acid-evoked bladder irritation in the anaesthetised female cat. *Br J Pharmacol*. 2006; 148: 154–61.
68. **Cardozo LD, Stanton SL, Robinson H, *et al.*** Evaluation of flurbiprofen in detrusor instability. *Br Med J*. 1980; 280: 281–2.
69. **Park JM, Houck CS, Sethna NF, *et al.*** Ketorolac suppresses postoperative bladder spasms after pediatric ureteral reimplantation. *Anesth Analg*. 2000; 91: 11–5.
70. **Delaere KP, Debruyne FM, Moonen WA.** The use of indomethacin in the treatment of idiopathic bladder instability. *Urol Int*. 1981; 36: 124–7.
71. **Chaudhuri TK, Fink S, Netto IC, *et al.*** Double-blind placebo controlled randomized trial of indomethacin on urodynamic values measured by radionuclide imaging. *Clin Auton Res*. 1993; 3: 37–40.